ONG: Orthogonal Natural Gradient Descent

Yajat Yadav
UC Berkeley
yajatyadav@berkeley.edu

Jathin Korrapati
UC Berkeley
jkorr@berkeley.edu

Patrick Mendoza
UC Berkeley
patmendoza6745@berkeley.edu

Abstract

Orthogonal gradient descent has emerged as a powerful method for continual learning tasks. However, its Euclidean projections overlook the underlying information-geometric structure of the space of distributions parametrized by neural networks, which can lead to suboptimal convergence in learning tasks. To counteract this, we combine it with the idea of the natural gradient and present **ONG (Orthogonal Natural Gradient Descent)**. ONG preconditions each new task gradient with an efficient EKFAC approximation of the inverse Fisher information matrix, yielding updates that follow the steepest descent direction under a Riemannian metric. To preserve performance on previously learned tasks, ONG projects these natural gradients onto the orthogonal complement of prior task gradients. We provide a theoretical justification for this procedure, introduce the ONG algorithm, and benchmark its performance on the Permuted and Rotated MNIST datasets. All code for our experiments/reproducibility can be found here at https://github.com/yajatyadav/orthogonal-natural-gradient.

1 Introduction

Continual learning, the process of training a single model on a sequence of tasks without forgetting previously learned tasks, is a big challenge in deep learning. Naive fine-tuning leads to an issue known as catastrophic forgetting, where earlier tasks' performance collapses as NNs shift their optimal parameters and weights to accommodate the new task, forgetting previously learned tasks [McCloskey and Cohen, 1989, Goodfellow et al., 2015]. In deep learning, a promising method to tackle this problem is orthogonal gradient descent. Orthogonal gradient descent proposes a solution where each new-task gradient is projected into an orthogonal subspace spanned by previous tasks' gradient steps. By subtracting off this projection before taking the gradient step, we ensure that the model predictions aren't affected by the trained parameters of previous tasks. Another idea in optimization is the natural gradient. Natural gradients arise when accounting for the underlying geometry of the parameter space in our optimization to find the steepest direction. Natural gradient descent has been found to require far fewer iterations than traditional gradient descent in many applications. It is also invariant to any smooth and invertible reparameterization of the model, as compared to gradient descent, which is parametrization dependent. Natural gradient descent works by modifying the gradient update rule to account for the "information geometry" of the parameter space. In the context of probabilistic models, this involves preconditioning the gradient in the update rule with the inverse Fisher information matrix, as it can be shown that the Riemannian metric structure of this parameter space is described by the Fisher information. This new formulation ensures optimization in the steepest descent direction. Our paper aims to incorporate natural gradients in the OGD algorithm to combine the strengths of these methods and create a robust continual learning algorithm. We present our algorithm, Orthogonal Natural Gradients (ONG), and provide some theoretical guarantees and an efficient implementation. We then test it on standard continual learning benchmarks.

Preprint. Under review.

2 Related Work

Continual Learning Methods Continual learning methods broadly fall into three categories: regularization-based, replay-based, and dynamic architecture methods. Regularization-based methods add task-specific penalties to the loss to preserve old knowledge. Notable works include Elastic Weight Consolidation [Kirkpatrick et al., 2017], which uses the Fisher information at a task's optimum as a quadratic penalty on parameter changes, and Synaptic Intelligence (SI) [Zenke et al., 2017], which integrates a Hebbian-like importance of each weight over tie. Memory Aware Synapses (MAS) compute parameter importance by measuring the sensitivity of the output function to each weight, and penalizes updates to important parameters [Aljundi et al., 2018]. All of these effectively "slow down" learning on critical weights after each task. Recent variants have hybridized and/or extended on these ideas [Schwarz et al., 2018, Loo et al., 2020, Batra and Clark, 2024]. Replay-based methods mitigate forgetting by rehearsing data from previous tasks during new-task training. This can be done by either storing real data or generating synthetic examples that approximate prior distributions. Deep Generative Replay (DGR) methods [Shin et al., 2017] train a generative model to mimic old data distributions. During new task training, the generative model samples pseudo-data from prior tasks, allowing the learner to "replay" previous experiences without storing real examples. Experience Replay (ER) [Rolnick et al., 2019] stores a subset of training samples from past tasks in a memory buffer and interleaves them with new data during learning. While effective, its drawbacks lie within concerns about memory usage and privacy. Further improvement include Prioritized Generative Replay [Wang et al., 2025] where random samples are generated condition on "relevance" functions, making samples richer and more informative than DGR. Hybrid approaches have also been proposed, combining replay and regularization [Prabhu et al., 2020, Yan et al., 2021]. Finally, dynamic architecture methods seek to address catastrophic forgetting by modifying the model structure over time, often by allocating task-specific sub-modules or expanding capacity to accommodate new tasks. Progressive Neural Networks (PNNs) [Rusu et al., 2022] allocate a new column for each task and connect it previous columns via lateral connections. This guarantees no forgetting but scales poorly with the number of tasks. Dynamically Expandable Networks (DEN) [Yoon et al., 2018] grow the network only when necessary, by splitting and duplicating neurons based on task specific losses, allowing for more compact architecture compared to PNNs. Similarly, PackNet [Mallya and Lazebnik, 2018] prunes a large model after each task and reuses freed weights for new tasks, enabling weight reuse without interference. Other dynamic methods use conditional computation or gating mechanisms to route different tasks through different subsets of the network, as in Context-dependent Gating [Masse et al., 2018], which applies task-specific masks over weights to isolate task representations. A notable continual learning method, one of which forms the foundation upon which our work builds and extends on, is Orthogonal Gradient Descent (OGD), originally proposed by Farajtabar et al. [2019]. OGD mitigates forgetting by projecting incoming gradients onto the orthogonal complement of the subspace spanned by previously observed gradients. Follow-up work by Bennani et al. [2020] offers theoretical guarantees for OGD in the neural tangent kernel (NTK) regime, demonstrating that under mild assumptions, OGD can preserve task performance indefinitely.

Natural Gradient Methods The natural gradient [Amari, 1998] generalizes standard gradient descent by taking steps that respect the geometry of the parameter space. Instead of updating parameters in the Euclidean space, natural gradients optimize in the space of probability distributions using the Fisher information matrix (FIM) as a Riemannian metric. In probabilistic models and Bayesian neural networks, natural gradient descent yields faster convergence and more stable updates by accounting for parameter sensitivity [Khan and Lin, 2017, Martens, 2020]. Methods such as Variational Online Gauss-Newton (VOGN) [Khan and Lin, 2017] and Bayesian Gradient Descent [Liu et al., 2023] utilize natural gradients for continual learning by updating variational parameters using FIM-preconditioned gradients. This is conceptually similar to OGD's gradient projection, in that both methods transform the gradient based on local curvature or constraints, aiming to minimize forgetting.

Efficient Approximations to Fisher Information While natural gradient methods are theoretically appealing, computing and inverting the full Fisher information matrix is often intractable for deep networks. To address this, several efficient approximations have been proposed: Diagonal approximations (as in standard EWC) are simple but ignore parameter interactions. Kronecker-Factored Approximate Curvature (K-FAC) [Martens, 2020] factorizes the FIM into smaller Kronecker com-

ponents, significantly reducing storage and compute requirements. EK-FAC (Eigenvalue-Corrected K-FAC) [George et al., 2018] improves on K-FAC by computing the eigenbasis of each factor and tracking variances in that space. This method provably offers a closer approximation to the true FIM in the Frobenius norm while retaining computational efficiency. Ritter et al. [2018] allow continuous curvature estimation using block-diagonal structures, further aiding in scalability for continual learning.

3 Preliminaries

3.1 Continual Learning

In continual learning, a model encounters tasks $\mathcal{T}_1, \mathcal{T}_2, \mathcal{T}_3, ...$ sequentially, each of which describes their own supervised learning task. Once the data task for $\mathcal{T}_k$ has been utilized for training, it is usually discarded (each example is seen once). The challenge of this method lies in updating the model so that it performs well on the current task without sacrificing its ability to solve all previously learned tasks [Nguyen et al., 2017]. Formally, we assume that for each task $\mathcal{T}_k$, the data $\{(\boldsymbol{x}_{k,i}, y_{k,i})\}_{i=1}^{n_k}$ are drawn i.i.d. from some distribution $\mathcal{D}_k$ [Bennani et al., 2020]. We denote the model parameters after t iterations on task k by $f_k^{(t)}$, and then use f_k^* to refer to the final parameters once the model learns the task [Tang et al., 2020].

3.2 Probabilistic Setup

When we train a neural network for classification, we implicitly fit a parametric family of probability distributions over the class labels. More formally, a multi-layer perceptron with softmax outputs defines

$$p\left(y \mid \boldsymbol{x}; \boldsymbol{w}\right) = \frac{\exp(f_y(\boldsymbol{x}; \boldsymbol{w}))}{\sum_{\mathrm{c}} \exp(f_{\mathrm{c}}(\boldsymbol{x}; \boldsymbol{w}))} \tag{1}$$

where $f_{\mathrm{c}}(\boldsymbol{x}; \boldsymbol{w})$ is the logit class for c. Our objective is to maximize the log-likelihood (equivalent to minimizing cross-entropy) so the learning problem lives on the manifold of all these predictive distributions. This is what motivates the use of the Fisher information matrix [Amari, 1998]:

$$\boldsymbol{F}(\boldsymbol{w}) = \mathbb{E}_{\boldsymbol{x} \sim \mathcal{D},\ y \sim p(y \mid \boldsymbol{x}; \boldsymbol{w})} \left[\nabla_{\boldsymbol{w}} \log p\left(y \mid \boldsymbol{x}; \boldsymbol{w}\right) \cdot \nabla_{\boldsymbol{w}} \log p\left(y \mid \boldsymbol{x}; \boldsymbol{w}\right)^{\top} \right] \tag{2}$$

Note that "Riemannian structure is given to the parameter space of multilayer networks by the Fisher information matrix" as found from Amari [1998]. Intuitively, $\boldsymbol{F}(\boldsymbol{w})$ measures the sensitivity of the model's output distribution to small changes in each parameter direction. Directions that correspond to large Fisher curvature produce large changes in the predictive distribution (which also implies a large KL divergence between the old and new probability distributions after taking a step in parameter space), while the "flat" directions do not affect the model's behavior much. This geometric structure on our parameter space motivates the natural gradient

$$\delta = \boldsymbol{F}^{-1}(\boldsymbol{w}) \nabla_{\boldsymbol{w}} \mathcal{L}(\boldsymbol{w}) \tag{3}$$

as being the steepest-descent direction of loss function $\mathcal{L}(\boldsymbol{w})$ over our manifold. The preconditioning by the inverse Fisher matrix also provides us with optimization steps that are invariant to model reparameterization, which can be useful in tasks such as classification [Martens, 2020].

3.3 Orthogonal Gradient Descent

In continual learning, Orthogonal Gradient Descent (OGD) is a method that aims to prevent forgetting by projecting each new task gradient onto a subspace spanned by previous task gradients, in order to retain performance on previously seen tasks. We begin by restating the original algorithm and then summarize its key theoretical guarantees.

Algorithm 1 Orthogonal Gradients Descent

Input: Task sequence $\mathcal{T}_1, \mathcal{T}_2, \mathcal{T}_3, \ldots$, learning rate η
Output: The optimal parameter $\boldsymbol{w}$
Initialize $S \leftarrow \{\}$; $\boldsymbol{w} \leftarrow \boldsymbol{w}_0$
for Task ID $k = 1, 2, 3, \ldots$ **do**
    repeat
        $\boldsymbol{g} \leftarrow$ Stochastic/Batch Gradient for $\mathcal{T}_k$ at $\boldsymbol{w}$
        $\tilde{\boldsymbol{g}} = \boldsymbol{g} - \sum_{\boldsymbol{v} \in S} \text{proj}_{\boldsymbol{v}}(\boldsymbol{g})$
        $\boldsymbol{w} \leftarrow \boldsymbol{w} - \eta \tilde{\boldsymbol{g}}$
    until convergence
    for $(\boldsymbol{x}, y) \in T_k$ and $k \in [1, c]$ such that $y_k = 1$ **do**
        $\boldsymbol{u} \leftarrow \nabla f_k(\boldsymbol{x}; \boldsymbol{w}) - \sum_{\boldsymbol{v} \in S} \text{proj}_{\boldsymbol{v}} \left(\nabla f_k(\boldsymbol{x}; \boldsymbol{w})\right)$
        $S \leftarrow S \cup \{\boldsymbol{u}\}$
    end for
end for

The above algorithm is the original OGD algorithm Farajtabar et al. [2019]. To justify the use of orthogonal gradient descent, it has been shown that every model update $\tilde{\boldsymbol{g}}$ remains a valid descent direction and that the generalization gap can be bounded just as tightly as it is for SGD [Bennani et al., 2020]. The forgetting bound is also tightly controlled by a factor that can limit how much any one past task's loss can rise. Together, these results show that OGD is not just empirically effective, but also comes with provable convergence, bounded generalization error, and guaranteed forgetting control Farajtabar et al. [2019]. All these aspects make it theoretically sound and appealing for continual learning and our applications with the natural gradient.

4 Method

We now describe our methodology to combine the core ideas of OGD and natural gradients to create a new continual learning algorithm ONG: Orthogonal Natural Gradient. This algorithm combines the parameter space invariant updates of natural gradients with the interference-free projections of orthogonal gradient descent (OGD). The key idea is partitioned into several steps.

4.1 Natural Preconditioning

For each new task gradient, $\boldsymbol{g} = \nabla_{\boldsymbol{w}} \mathcal{L}_{T_k}$, we edit this gradient to instead be

$$\boldsymbol{g} = \boldsymbol{F}^{-1} \nabla_{\boldsymbol{w}} \mathcal{L}_{T_k} \tag{4}$$

where $\boldsymbol{F}$ is the approximate Fisher information matrix, estimated for the current set of model parameters. This step moves the parameters $\boldsymbol{w}$ along the steepest direction on the manifold of the predictive distributions, which minimizes the KL-divergence from the conditional distribution parameterized by the previous model and ensures reparameterization invariance. The remaining steps from the previous algorithm remain the same. We still maintain a basis S of "sensitive" directions and project $\boldsymbol{g}$ into the orthogonal complement of the span of S:

$$\tilde{\boldsymbol{g}} = \boldsymbol{g} - \sum_{\boldsymbol{v} \in S} \text{proj}_{\boldsymbol{v}}(\boldsymbol{g}) \tag{5}$$

We perform the same parameter update

$$\mathbf{w} \;\leftarrow\; \mathbf{w} - \eta\, \tilde{\mathbf{g}},$$

and once task T_k converges—just as in the OGD paper—we extract each logit-wise gradient $\nabla f_k(\boldsymbol{x}; \boldsymbol{w})$. Then, as before, we precondition this gradient, project it onto the orthogonal complement of the subspace spanned by all previously added logit-wise gradients, and denote the result by $\boldsymbol{u}$. Finally, we add $\boldsymbol{u}$ to our set S, maintaining S as an orthogonal basis of "sensitive directions." S spans the subspace of all previously seen *natural* gradients.

4.2 OGD-Plus (OGD+)

OGD-Plus(OGD+) is an algorithm that enhances vanilla OGD by storing the feature maps w.r.t samples from previous tasks, in addition to feature maps w.r.t samples from current task (which is what OGD stores) [Bennani et al., 2020]. These extra samples are saved in a dedicated memory, the sample memory. The authors motivated this change in order to make OGD more robust to the NTK (Neural Tangent Kernel) variation phenomena in the experiments. The changes from OGD to OGD+ can be found in blue in the below algorithm.

Algorithm 2 ONG / ONG+

Input: Task sequence $\mathcal{T}_1, \mathcal{T}_2, \mathcal{T}_3, \ldots$, learning rate η
Output: The optimal parameter $\boldsymbol{w}$
Initialize $S \leftarrow \{\}$; $S_D \leftarrow \{\}$; $\boldsymbol{w} \leftarrow \boldsymbol{w}_0$
for Task ID $k = 1, 2, 3, \ldots$ **do**
  repeat
    $\boldsymbol{g} \leftarrow$ Stochastic/Batch Gradient for $\mathcal{T}_k$ at $\boldsymbol{w}$
    $\boldsymbol{g} \leftarrow \boldsymbol{F}^{-1}\boldsymbol{g}$
    $\tilde{\boldsymbol{g}} = \boldsymbol{g} - \sum_{\boldsymbol{v} \in S} \text{proj}_{\boldsymbol{v}}(g)$
    $\boldsymbol{w} \leftarrow \boldsymbol{w} - \eta\tilde{\boldsymbol{g}}$
  until convergence
  Sample $H \subset S_D$
  for $(\boldsymbol{x}, y) \in T_k \cup H$ and $k \in [1, c]$ such that $y_k = 1$ **do**
    $u \leftarrow \boldsymbol{F}^{-1}\nabla f_k(\boldsymbol{x}; \boldsymbol{w}) - \sum_{\boldsymbol{v} \in S} \text{proj}_{\boldsymbol{v}} (\nabla f_k(\boldsymbol{x}; \boldsymbol{w}))$
    $S \leftarrow S \cup \{\boldsymbol{u}\}$
  end for
  Sample $D \subset T_k$
  Update $S_D \leftarrow S_D \cup D$
end for

4.3 ONG and ONG+

In this paper, we present ONG and ONG+, extensions of OGD and OGD+ using natural gradients, respectively. Our changes are in red in algorithm 2: we essentially precondition gradients using the Fisher information matrix both when updating model parameters and when storing task gradients in memory (the span of this set is what future gradients are ultimately projected onto).

4.4 Theoretical Guarantees

This section focuses on studying the ONG algorithm (aka Algorithm 2 without the blue text) to obtain some theoretical results. Analogous to Lemma 3.1 from the original OGD paper [Farajtabar et al., 2019], we present a proof that the preconditioned, projection-subtracted gradient $\tilde{\boldsymbol{g}}$ is still a descent direction with respect to the Fisher metric.

As described in section 3.1, in the context of probabilistic models, the Riemannian metric tensor is the Fisher information matrix $\boldsymbol{F}$ in model parameter space. Theorem 1 from Farajtabar et al. [2019] highlights that in this Riemannian manifold, $-\boldsymbol{F}^{-1}\nabla\mathcal{L}(\boldsymbol{w})$ is the steepest descent direction of the loss. Thus, if $\langle\tilde{\boldsymbol{g}}, -\boldsymbol{F}^{-1}\nabla_{\boldsymbol{w}}\mathcal{L}(\boldsymbol{w})\rangle \leq 0$, $\tilde{\boldsymbol{g}}$ will be a valid descent direction w.r.t the metric structure of the manifold as well. The following lemma proves this.

Lemma 4.1. *Let $\boldsymbol{F}^{-1}\boldsymbol{g}$ be the natural gradient of loss function $\mathcal{L}(\boldsymbol{w})$ and $S = \{\boldsymbol{v}_1, \ldots, \boldsymbol{v}_n\}$ be the orthogonal basis. Define $\tilde{\boldsymbol{g}} = \boldsymbol{F}^{-1}\boldsymbol{g} - \sum_i^k \text{proj}_{\boldsymbol{v}_i}(\boldsymbol{F}^{-1}\boldsymbol{g})$, where $\text{proj}_{\boldsymbol{v}_i}(\boldsymbol{F}^{-1}\boldsymbol{g})$ denotes the projection of $\boldsymbol{F}^{-1}\boldsymbol{g}$ onto the $\boldsymbol{v}_i$. Then, $-\tilde{\boldsymbol{g}}$ is also a descent direction for $\mathcal{L}(\boldsymbol{w})$, with respect to the metric structure of the model parameter space.*

Proof. For $-\tilde{\boldsymbol{g}}$ to be a valid descent direction it should satisfy $\langle -\tilde{\boldsymbol{g}}, \boldsymbol{F}^{-1}\boldsymbol{g}\rangle \leq 0$. We have

$$\langle -\tilde{\boldsymbol{g}},\ \boldsymbol{F}^{-1}\boldsymbol{g}\rangle = \langle -\tilde{\boldsymbol{g}}, \tilde{\boldsymbol{g}} + \sum_{i=1}^{k} \mathrm{proj}_{\boldsymbol{v}_i}(F^{-1}\boldsymbol{g})\rangle \tag{6}$$

$$= -\|\tilde{\boldsymbol{g}}\|^2 - \langle \tilde{\boldsymbol{g}}, \sum_{i=1}^{k} \mathrm{proj}_{\boldsymbol{v}_i}(\boldsymbol{F}^{-1}\boldsymbol{g})\rangle\ . \tag{7}$$

Since $\tilde{\boldsymbol{g}} = \boldsymbol{F}^{-1}\boldsymbol{g} - \sum_{i=1}^{k} \mathrm{proj}_{\boldsymbol{v}_i}(\boldsymbol{F}^{-1}\boldsymbol{g})$ is orthogonal to the space spanned by the vectors in S and each $\mathrm{proj}_{\boldsymbol{v}_i}(\boldsymbol{F}^{-1}\boldsymbol{g})$ lies in this space, $\tilde{\boldsymbol{g}}$ will be orthogonal to $\sum_{i=1}^{k} \mathrm{proj}_{\boldsymbol{v}_i}(\boldsymbol{F}^{-1}\boldsymbol{g})$. Thus, $\langle \tilde{\boldsymbol{g}}, \sum_{i=1}^{k} \mathrm{proj}_{\boldsymbol{v}_i}(\boldsymbol{F}^{-1}\boldsymbol{g})\rangle = 0$. Substituting this into Eq. 7, we arrive at $\langle -\tilde{\boldsymbol{g}},\ \boldsymbol{F}^{-1}\boldsymbol{g}\rangle = -\|\tilde{\boldsymbol{g}}\|^2 \leq 0$. Therefore, $-\tilde{\boldsymbol{g}}$ is a valid descent direction for $\mathcal{L}(\boldsymbol{w})$ while being perpendicular to S. □

4.5 EKFAC Fisher Approximation

Calculating the exact Fisher matrix is computationally expensive, making it far too large to use and invert scaling up to millions of parameters with certain neural network models per. A nice compromise between full natural gradient and simple diagonal scaling is the Eigenvalue-corrected Kronecker Factorization (EKFAC) [George et al., 2018]. EKFAC works by providing a diagonal approximation not in the raw parameter basis, but in the Kronecker-factored eigenbasis, where a diagonal captures most of the curvature information at a very low cost. Each layer's Fisher block is approximated as $\boldsymbol{F} = \boldsymbol{A} \otimes \boldsymbol{B}$ with the Kronecker factors $\boldsymbol{A} = \boldsymbol{Q_A}\boldsymbol{\Lambda_A}\boldsymbol{Q_A}^\top \boldsymbol{B} = \boldsymbol{Q_B}\boldsymbol{\Lambda_B}\boldsymbol{Q_B}^\top$ and then tracks the diagonal $\boldsymbol{\Lambda_A}$ and $\boldsymbol{\Lambda_B}$ in that eigenbasis, so each mini-batch update is just two small eigentransforms plus a diagonal rescaling. We utilize this approximation of the Fisher matrix in our code implementation. Note that to force the Fisher matrix to be PD, we add $\lambda \boldsymbol{I}$ to it in order to force the fisher matrix to be invertible and numerically more stable in training. We adapt the EKFAC algorithm [Vantanapath and contributors, 2020] in our method, leading to faster and more stable training.

5 Experiments

5.1 Datasets

We evaluate our method on two standard benchmark datasets utilized extensively in continual learning literature: Permuted MNIST and Rotated MNIST.

5.1.1 Permuted MNIST

Permuted MNIST generates K tasks by fixing K independent random permutations of the 784 input pixels. Each task are the original MNIST images with its pixels reshuffled by one of those permutations, forcing the model to learn to classify under radically different orderings without forgetting prior permutations.

5.1.2 Rotated MNIST

Rotated MNIST applies a fixed rotation angle θ_k to every MNIST digit. At task k, all training and test images are rotated by θ_k, which forces the model to continually adapt to new orientations while remembering earlier orientations with different angles.

5.2 Evaluation Criteria

For evaluation purposes, we adapt the same metrics as Bennani et al. [2020]: average accuracy and average forgetting. Let $a_{\mathcal{T},k}$ denote the accuracy of the model on the $\mathcal{T}_k$ after being trained on the task $\mathcal{T}$.

5.2.1 Average Accuracy

Average accuracy (A_T) is the accuracy of the model after its trained on task $\mathcal{T}_T$. It is defined as:

$$A_T = \frac{1}{T}\sum_{k=1}^{T} a_{T,k} \tag{8}$$

5.2.2 Average Forgetting

Average forgetting (F_T) is the average forgetting the model has after its been trained on task $\mathcal{T}_T$. It is defined as:

$$F_T = \frac{1}{T-1}\sum_{k=1}^{T-1} \max_{t\in\{1,\dots T-1\}} (a_{t,k} - a_{T,k}) \tag{9}$$

5.3 Setup

We use a base model of a three-layer MLP with 100 hidden units in two layers, with about 115,000 total parameters. Each layer uses RELU activation, and the final output are the 10 logits.

After some experimentation, we settle on 3 epochs per task, a learning rate of 0.001, a memory buffer size of 100 samples per task, and batch size 32. The seeds ranged from 0 to 5. No training augmentations were added, and this could be part of a future follow-up. All training and validation was done on 1 NVIDIA A100.

The training step logic was modified to keep track of the running estimates needed for the EKFAC algorithm. The optimizer step logic was modified to efficiently use EKFAC for preconditioning the gradient vector.

5.4 Results

5.4.1 Forgetting and Average Validation Accuracy

Here, we look at the average forgetting and average validation accuracy, as described above, of the two baseline methods (OGD and OGD+), as well as our natural gradient extensions to each (ONG and ONG+). Table 1 highlights the average forgetting values, while Table 2 highlights the final average validation accuracy.

Table 1: The average forgetting of all the methods we considered (lower is better).

Dataset	Permuted MNIST	Rotated MNIST
OGD	4.1534	16.1282
OGD+	1.0563	6.0064
ONG	58.7240	28.7360
ONG+	57.5692	27.6238

Table 2: The final validation accuracy, averaged over all tasks, of all the methods we considered.

Dataset	Permuted MNIST	Rotated MNIST
OGD	82.6604	77.7443
OGD+	85.8746	87.6950
ONG	32.5053	69.0968
ONG+	33.5723	70.1771

5.4.2 Permuted MNIST

Here, we more closely examine our methods' performance on Permuted MNIST. Table 3 lists the final task-wise test accuracies for each method after the model finishes sequentially training on all tasks. The plots in Figure 1 examine the evolution of validation accuracy during training, specifically how per-task accuracies evolve as the model continues to be trained on newer and newer tasks.

Table 3: Permuted MNIST: Test accuracy of each method on the indicated task after training sequentially on all tasks.

(a) Tasks 1 – 7

Model	Accuracy						
	Task 1	Task 2	Task 3	Task 4	Task 5	Task 6	Task 7
OGD	38.91	68.55	71.73	79.71	83.41	87.27	85.83
OGD+	74.69	76.57	76.12	79.42	82.03	84.72	85.16
ONG	5.44	10.22	17.08	14.24	8.17	12.88	15.74
ONG+	13.64	16.48	15.44	16.26	11.00	14.39	19.69

(b) Tasks 8 – 15

Model	Accuracy							
	Task 8	Task 9	Task 10	Task 11	Task 12	Task 13	Task 14	Task 15
OGD	87.26	88.79	88.59	89.93	91.56	92.02	92.96	93.39
OGD+	87.91	89.03	90.56	90.74	91.92	92.74	93.11	93.39
ONG	23.73	24.75	25.89	44.99	40.09	66.53	81.48	96.35
ONG+	23.86	26.40	33.47	29.67	43.95	54.85	88.15	96.34

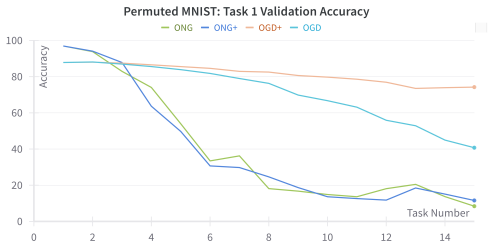

(a) Task 1 accuracy throughout tasks

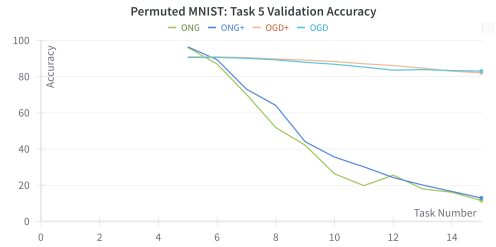

(b) Task 5 accuracy throughout tasks

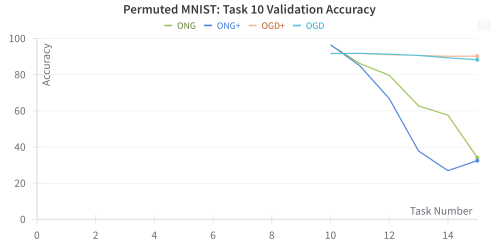

(c) Task 10 accuracy throughout tasks

Figure 1: Validation Accuracy for tasks 1, 5, and 10 of the Permuted MNIST dataset throughout training. The model is sequentially trained on tasks 1 through 15, and thus the x-axis is presented in terms of number of tasks.

5.4.3 Rotated MNIST

Here, we more closely examine our methods' performance on Rotated MNIST. Table 4 lists the final task-wise test accuracies for each method after the model finishes sequentially training on all tasks. The plots in Figure 2 examine the evolution of validation accuracy during training, specifically how per-task accuracies evolve as the model continues to be trained on newer and newer tasks.

Table 4: Rotated MNIST: Test accuracy of each model on the indicated task after training sequentially on all tasks.

(a) Tasks 1 – 7

Model	Accuracy						
	Task 1	Task 2	Task 3	Task 4	Task 5	Task 6	Task 7
OGD	41.83	43.75	53.89	61.19	68.45	74.93	82.01
OGD+	69.67	73.21	79.06	83.27	85.71	86.87	89.59
ONG	24.42	27.60	34.24	41.48	49.81	58.32	67.85
ONG+	27.59	30.30	37.41	43.31	51.86	59.68	68.94

(b) Tasks 8 – 15

Model	Accuracy							
	Task 8	Task 9	Task 10	Task 11	Task 12	Task 13	Task 14	Task 15
OGD	85.49	89.33	91.97	93.39	94.83	95.03	95.27	94.80
OGD+	90.15	91.91	92.95	93.74	94.83	95.15	94.92	94.40
ONG	75.81	84.03	90.02	93.88	96.41	97.17	97.74	97.68
ONG+	77.10	84.27	89.58	93.64	96.23	97.39	97.58	97.78

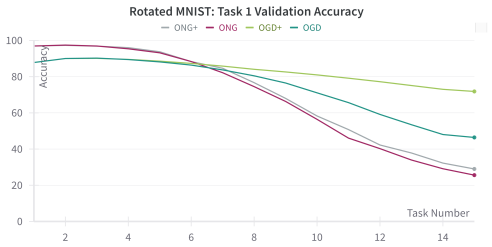

(a) Task 1 accuracy throughout tasks

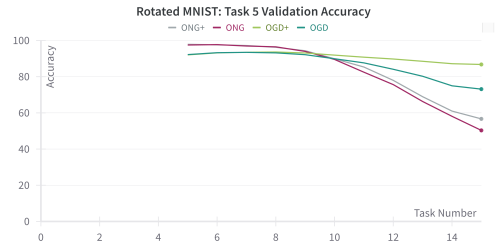

(b) Task 5 accuracy throughout tasks

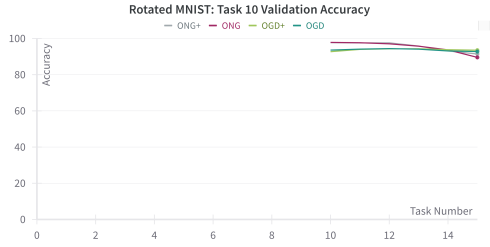

(c) Task 10 accuracy throughout tasks

Figure 2: Validation Accuracy for tasks 1, 5, and 10 of the Rotated MNIST dataset throughout training. The model is sequentially trained on tasks 1 through 15, and thus the x-axis is presented in terms of number of tasks.

6 Conclusion and Outlook

In this paper, we introduce a new continual learning algorithm, ONG, that combines the interference-free subspace projections of OGD with the information geometry preconditioning of the natural gradient. We prove ONG retains the descent-direction guarantees under the Fisher metric, and how to implement it using the EKFAC fisher approximation method. However, interestingly enough ONG performed worse on the tasks of Permuted and Rotated MNIST, particularly on Permuted MNIST. While it was unable to outperform its continual learning counterpart in Euclidean space, these results highlight the challenges in combining Fisher preconditioning with orthogonal-projection-based methods.

Moving forward, an exciting way to improve ONG will be to incorporate more insights from the field of Manifold Learning and Information Geometry. One such idea is the concept of parallel transports. From Li and Ma [2022], we have the following definition.

Definition 1 (Parallel transport)**.** *Given a complete Riemannian manifold* $(\mathcal{M}, g)$ *and two points* $x, y \in \mathcal{M}$*, the* parallel transport

$$P_{x\to y} : T_x\mathcal{M} \longrightarrow T_y\mathcal{M}^1$$

is the linear isometry satisfying

$$\left\langle P_{x\to y}\,\xi,\ P_{x\to y}\,\zeta \right\rangle_y = \langle \xi, \zeta \rangle_x \quad \forall\, \xi, \zeta \in T_x\mathcal{M}.$$

As Budninskiy et al. [2018] further highlights, parallel transport provides a powerful way of connecting the geometries of nearby points in manifolds with non-trivial curvature. An exciting extension to ONG would be to utilize parallel transport with a well-chosen curve in order to "transport" all natural gradients into the same tangent space and use that space's inner product for projections and building the orthonormal basis.

Another exciting avenue for future study is to further explore the parameterization-invariance property. This was a major reason we chose natural gradients in this project, so future work studying which model reparameterizations ONG and similar natural-gradient-based methods remain robust to will be an interesting area of research.

Finally, Permuted MNIST and Rotated MNIST used in our experiments were toy datasets, and we believe it is important to analyze the various continual learning approaches with datasets consisting of more diverse, uncorrelated tasks. We hypothesize that the benefits of natural gradient-based methods will be more pronounced in such challenging setups.

[1] On a complete Riemannian manifold the geodesic between any two points is unique, so $P_{x\to y}$ is well-defined.

References

Rahaf Aljundi, Francesca Babiloni, Mohamed Elhoseiny, Marcus Rohrbach, and Tinne Tuytelaars. Memory aware synapses: Learning what (not) to forget, 2018. URL https://arxiv.org/abs/1711.09601.

Shun-ichi Amari. Natural gradient works efficiently in learning. *Neural Computation*, 10(2):251–276, 1998. doi: 10.1162/089976698300017746. URL https://direct.mit.edu/neco/article/10/2/251/6143/Natural-Gradient-Works-Efficiently-in-Learning.

Hunar Batra and Ronald Clark. Evcl: Elastic variational continual learning with weight consolidation, 2024. URL https://arxiv.org/abs/2406.15972.

Mehdi Abbana Bennani, Thang Doan, and Masashi Sugiyama. Generalisation guarantees for continual learning with orthogonal gradient descent. arXiv:2006.11942, 2020. URL https://arxiv.org/abs/2006.11942.

Max Budninskiy, Gloria Yin, Leman Feng, Yiying Tong, and Mathieu Desbrun. Parallel transport unfolding: A connection-based manifold learning approach. In *Symposium on Geometry Processing*, 2018. URL https://geometry.caltech.edu/pubs/BYFTD18.pdf.

Mehrdad Farajtabar, Navid Azizan, Alex Mott, and Ang Li. Orthogonal gradient descent for continual learning. arXiv:1910.07104, 2019. URL https://arxiv.org/abs/1910.07104.

Théo George, Emmanuel Marceau-Caron, Brendt Wohlberg, and Mark Sandler. Eigenvalue-corrected kronecker factorization for natural gradient descent. arXiv:1806.03884, 2018. URL https://arxiv.org/abs/1806.03884.

Ian J. Goodfellow, Mehdi Mirza, Da Xiao, Aaron Courville, and Yoshua Bengio. An empirical investigation of catastrophic forgetting in gradient-based neural networks, 2015. URL https://arxiv.org/abs/1312.6211.

Mohammad Emtiyaz Khan and Wu Lin. Conjugate-computation variational inference : Converting variational inference in non-conjugate models to inferences in conjugate models, 2017. URL https://arxiv.org/abs/1703.04265.

James Kirkpatrick, Razvan Pascanu, Neil Rabinowitz, Joel Veness, Guillaume Desjardins, Andrei A. Rusu, Kieran Milan, John Quan, Tiago Ramalho, Agnieszka Grabska-Barwinska, Demis Hassabis, Claudia Clopath, Dharshan Kumaran, and Raia Hadsell. Overcoming catastrophic forgetting in neural networks. *Proceedings of the National Academy of Sciences*, 114(13):3521–3526, March 2017. ISSN 1091-6490. doi: 10.1073/pnas.1611835114. URL http://dx.doi.org/10.1073/pnas.1611835114.

Jiaxiang Li and Shiqian Ma. Federated learning on riemannian manifolds, 2022. URL https://arxiv.org/abs/2206.05668. Manuscript.

Tianyi Liu, Yifan Lin, and Enlu Zhou. Bayesian stochastic gradient descent for stochastic optimization with streaming input data, 2023. URL https://arxiv.org/abs/2202.07581.

Noel Loo, Siddharth Swaroop, and Richard E. Turner. Generalized variational continual learning, 2020. URL https://arxiv.org/abs/2011.12328.

Arun Mallya and Svetlana Lazebnik. Packnet: Adding multiple tasks to a single network by iterative pruning, 2018. URL https://arxiv.org/abs/1711.05769.

James Martens. New insights and perspectives on the natural gradient method. *Journal of Machine Learning Research*, 21(146):1–76, 2020. URL http://jmlr.org/papers/v21/17-678.html.

Nicolas Y. Masse, Gregory D. Grant, and David J. Freedman. Alleviating catastrophic forgetting using context-dependent gating and synaptic stabilization. *Proceedings of the National Academy of Sciences*, 115(44), October 2018. ISSN 1091-6490. doi: 10.1073/pnas.1803839115. URL http://dx.doi.org/10.1073/pnas.1803839115.

Michael McCloskey and Neal J. Cohen. Catastrophic interference in connectionist networks: The sequential learning problem. volume 24 of *Psychology of Learning and Motivation*, pages 109–165. Academic Press, 1989. doi: https://doi.org/10.1016/S0079-7421(08)60536-8. URL https://www.sciencedirect.com/science/article/pii/S0079742108605368.

Cuong V. Nguyen, Yingzhen Li, Thang D. Bui, and Richard E. Turner. Variational continual learning. arXiv:1710.10628, 2017. URL https://arxiv.org/abs/1710.10628.

Ameya Prabhu, Philip H. S. Torr, and Puneet K. Dokania. Gdumb: A simple approach that questions our progress in continual learning. In *Computer Vision – ECCV 2020: 16th European Conference, Glasgow, UK, August 23–28, 2020, Proceedings, Part II*, page 524–540, Berlin, Heidelberg, 2020. Springer-Verlag. ISBN 978-3-030-58535-8. doi: 10.1007/978-3-030-58536-5_31. URL https://doi.org/10.1007/978-3-030-58536-5_31.

Hippolyt Ritter, Aleksandar Botev, and David Barber. Online structured laplace approximations for overcoming catastrophic forgetting, 2018. URL https://arxiv.org/abs/1805.07810.

David Rolnick, Arun Ahuja, Jonathan Schwarz, Timothy P. Lillicrap, and Greg Wayne. Experience replay for continual learning, 2019. URL https://arxiv.org/abs/1811.11682.

Andrei A. Rusu, Neil C. Rabinowitz, Guillaume Desjardins, Hubert Soyer, James Kirkpatrick, Koray Kavukcuoglu, Razvan Pascanu, and Raia Hadsell. Progressive neural networks, 2022. URL https://arxiv.org/abs/1606.04671.

Jonathan Schwarz, Jelena Luketina, Wojciech M. Czarnecki, Agnieszka Grabska-Barwinska, Yee Whye Teh, Razvan Pascanu, and Raia Hadsell. Progress & compress: A scalable framework for continual learning, 2018. URL https://arxiv.org/abs/1805.06370.

Hanul Shin, Jung Kwon Lee, Jaehong Kim, and Jiwon Kim. Continual learning with deep generative replay, 2017. URL https://arxiv.org/abs/1705.08690.

Haobo Tang, Xianzhi Song, Yingbo Li, Yue Zhang, Stephan Mandt, and Yifan Liu. Continual learning with bayesian neural networks for non-stationary data. arXiv:2006.11942, 2020. URL https://arxiv.org/abs/2006.11942.

Pattarapo Vantanapath and contributors. Natural gradient descent - examples and tutorials. https://github.com/wiseodd/natural-gradients, 2020. Accessed: 2024-05-15.

Renhao Wang, Kevin Frans, Pieter Abbeel, Sergey Levine, and Alexei A. Efros. Prioritized generative replay, 2025. URL https://arxiv.org/abs/2410.18082.

Shipeng Yan, Jiangwei Xie, and Xuming He. Der: Dynamically expandable representation for class incremental learning, 2021. URL https://arxiv.org/abs/2103.16788.

Jaehong Yoon, Eunho Yang, Jeongtae Lee, and Sung Ju Hwang. Lifelong learning with dynamically expandable networks, 2018. URL https://arxiv.org/abs/1708.01547.

Friedemann Zenke, Ben Poole, and Surya Ganguli. Continual learning through synaptic intelligence, 2017. URL https://arxiv.org/abs/1703.04200.